Available online at www.sciencedirect.com
SCIENCE DIRECT®
Journal of Pharmaceutical and Biomedical Analysis
31 (2003) 271–281
JOURNAL OF PHARMACEUTICAL AND BIOMEDICAL ANALYSIS
www.elsevier.com/locate/jpba

# Structural studies on the impurities of troglitazone

J. Moses Babu [a], D. Nageshwar [b], Y. Ravindra Kumar [a], C. Prabhakar [b], M.R. Sarma [b], G. Om Reddy [b], K. Vyas [a,*]

[a] *Department of Analytical Research, Discovery Research Division, Dr. Reddy's Laboratories Ltd., Bollaram Road, Miyapur, Hyderabad 500050, India*

[b] *Technology Development Center, Custom Chemical Services, Dr. Reddy's Laboratories Ltd., Bollaram Road, Miyapur, Hyderabad 500050, India*

Received 28 June 2002; received in revised form 27 October 2002; accepted 1 November 2002

**Abstract**

The impurity profile study of troglitazone has been carried out primarily by (liquid chromatography–mass spectrometry) LC–MS. Four process-related impurities have been detected by LC–MS and were confirmed by co-injection with authentic samples. Apart from the process-related impurities, two polar by-products were characterized by mass spectral data and comparison with reference samples, while one non-polar by-product and one degradation product have been isolated by means of preparative HPLC and characterized by 2D NMR and mass spectral study. Single-crystal X-ray diffraction studies have been carried out on the degradation product. The formation and characterization of these by-products and degradation product are discussed.


*Keywords:* Troglitazone; Impurities; LC–MS; NMR; Identification and characterization

## 1. Introduction

In non-insulin-dependent diabetes mellitus (NIDDM), a decrease in insulin effectiveness leads to hyperglycemia. This decrease in insulin action is related to impaired secretion, peripheral insulin resistance, and increased hepatic glucose production. In conventional treatment of NIDDM, sulphonyl urea drugs (SU drugs) have principally been used as oral hypoglycemic drugs to stimulate insulin secretion. However, it has been pointed out clinically that this kind of treatment aggravates the disease, due to fatigue of the pancreatic β-cells, increase in secondary failure of efficacy during long-term treatment, enhancement of obesity by insulin in obese patients, and a high possibility of hypoglycemia. Due to these problems, major challenge in this field has been to develop a pharmacological therapy, which can reduce peripheral insulin resistance and/or decrease hepatic glucose production. As a result of sustained research in this area, troglitazone [1] has emerged as a clinically useful hypoglycemic drug for NIDDM patients inadequately responding to diet

* Corresponding author. Fax: +91-40-304-5438.
*E-mail address:* vyask@drreddys.com (K. Vyas).

0731-7085/03/$ - see front matter 
doi:10.1016/S0731-7085(02)00665-9

or SU drug therapy, with completely different mechanism of action to those of conventional SU drugs. In view of the importance of troglitazone and our own interest [2,3] in the antidiabetic drug arena, we attempted the study of impurity profile of the drug substance. The preparation of troglitazone has been carried out employing scheme 1 using known methods [4] making only a few modifications to make it simple and commercially viable.

## 2. Experimental

### 2.1. Chemicals

Analytical reagent grade ammonium acetate was purchased from SD fine chemicals. HPLC grade methanol and acetonitrile were from Merck, USA. High pure Milli Q water was used with the help of Millipore milliQ plus purification system.

### 2.2. Samples

Troglitazone was recrystallized from methanol. The mother liquor containing the impurities was used for the (liquid chromatography–mass spectrometry) LC–MS analysis and isolation of two new impurities by chromatographic techniques.

### 2.3. Equipment

#### 2.3.1. Liquid chromatography–mass spectrometry

The LC–MS analysis was done on HP-5989A mass spectrometer with 59980B particle beam interface with HP-1050 HPLC pump. The mass spectrometer was operated with ionization electron beam energy of 70 eV. Source and quadrupole temperatures maintained at 250 and 100 °C, respectively. In the particle beam interface, the helium pressure was kept at 50 psi and the Nebulizer setting at 4. A Hypersil BDS C18 ($250 \times 4.6$ mm$^2$) 5 μm column was used with a mobile phase (0.05 M $CH_3COONH_4$:$CH_3CN$:$CH_3OH$, 33:55:12, pH 4.5) at the flow rate of 0.6 ml/min. A Shimadzu UV detector was also used to monitor the LC parallel at 254 nm.

#### 2.3.2. NMR studies

$^1$H and $^{13}$C NMR studies were done at 200 and 50 MHz, respectively, in $CDCl_3$ on a Varian Gemini 200 MHz FT NMR spectrometer. $^1$H and $^{13}$C chemical shifts are reported on the $\delta$ scale in ppm, relative to TMS ($\delta = 0.00$) and $CDCl_3$ ($\delta = 77.0$), as internal standard. DEPT spectral editing revealed the presence of methyl and methine groups as positive peaks while the methylenes as negative peaks. The exchangeable protons were identified by $D_2O$ exchange.

## 3. Experimental

### 3.1. Preparation of troglitazone

Esterification of Trolox 1 (182 g, 0.728 M) employing conventional methods affords 190 g (yield: 98%; HPLC purity: 98%; m.p.: 154–158 °C) of ester **2**. Ester **2** (100 g, 0.379 M) on reduction using sodium borohydride (36 g, 0.947 M) yields 88 g (yield: 98%; HPLC purity: 97%; m.p.: 108–110 °C) of alcohol **3**. MOM protection of alcohol **3** (100 g, 0.424 M) gives 112 g (yield: 94%; HPLC purity: 81%) of the protected alcohol **4** as an oily material which is used as such for the next step without any further purification. Mesylation of the MOM-protected alcohol **4** (112 g, 0.40 M) affords 117 g (yield: 77% based on alcohol **3**; HPLC purity: 93%; m.p.: 90–96 °C) of mesylate **5**. Condensation of mesylate **5** (115 g, 0.321 M) with 4-hydroxybenzaldehyde (61 g, 0.5 M) yields 117 g (yield: 94%; HPLC purity: 76%) of aldehyde **6** as an oily material. Aldehyde **6** (117 g, 0.307 M) upon reaction with thiazoldine-2,4-dione (34 g, 0.291 M) in the presence of benzoic acid (3.5 g, 0.029 M) and piperidine (3 g, 0.035 M) yields compound **7** (wt.: 234 g; HPLC purity: 77%) which is used for the next step without any further purification. The MOM-protected compound **7** (219 g, 0.453 M) is deprotected with 10% hydrochloric acid in methanol (500 ml) to give compound **8** (wt.: 96 g; yield: 68% based on mesylate **5**; HPLC purity: 96%). The unsaturated compound **8** (81 g, 01845 M) is reduced using Mg/methanol, followed by recrystallization from methanol to afford 40 g (yield: 50%; HPLC purity: 99.5%; m.p.:

175–177 °C) of troglitazone **9** as a white solid. The methanol mother liquors enriched with the impurities are used for the impurity profile study. Scheme for the synthesis of troglitazone is shown in Fig. 1.

### 3.2. Preparation of an authentic sample of *10*

The MOM-protected mesylate **5** (10 g, 27.9 mM) is taken in 50 ml of 10% hydrochloric acid in methanol and stirred at room temperature for a period of 2 h. The progress of the reaction is monitored by TLC. After the completion of the reaction, methanol is removed under reduced pressure at room temperature and the aq. layer is extracted into dichloromethane. The combined organic layer is concentrated to afford the deprotected mesylate **10** (7.5 g; yield: 85%; m.p.: 135–137 °C).

### 3.3. Preparation of an authentic sample of *11*

To diol **3** (10 g, 42 mM), dissolved in 100 ml of dichloromethane, is added sodium bromide (2.1 g, 21 mM) dissolved in 25 ml of water. The mixture is cooled to 0 °C and TEMPO (2 mg) is added followed by a slow addition of a mixture of sodium hypochlorite (20% (w/v), 77 ml, 0.21 M), sodium bicarbonate (4.8 g, 57 mM) and 10 ml of water at 0–5 °C. The reaction mixture is stirred at the same temperature for further 30 min and the progress of the reaction is monitored by TLC. After completion of the reaction, sodium thiosulphate (2.6 g, 11 mM) dissolved in 20 ml of water is added and stirred for 10 min at 0 °C. The organic

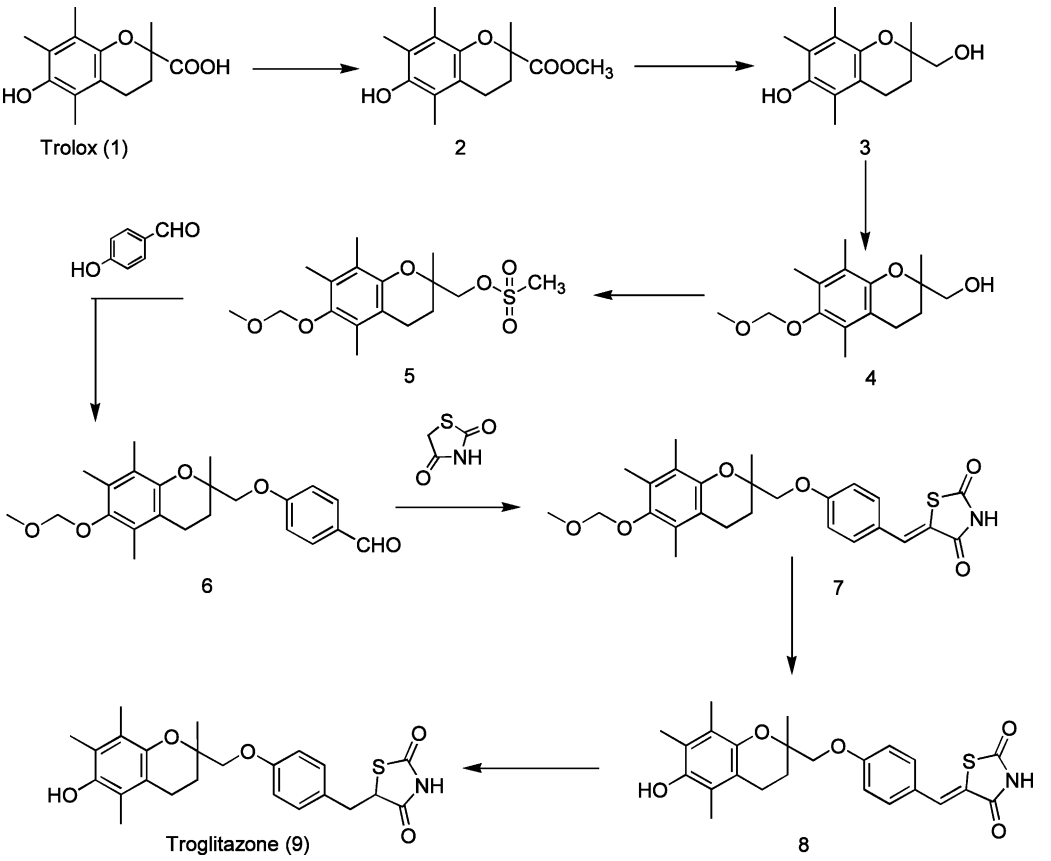


Fig. 1. Synthetic scheme of troglitazone.

Table 1

| Compound | Ret. time | Molecular ion | Structure | Confirmed by | Classification |
|---|---|---|---|---|---|
| **3** | 8.5 | 236 | 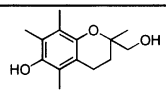 | Co-injection | Process Intermediate |
| **10** | 9.9 | 314 | 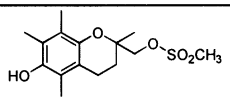 | MS data | Byproduct |
| **2** | 12.0 | 264 | 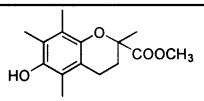 | Co-injection | Process Intermediate |
| **4** | 12.9 | 280 | 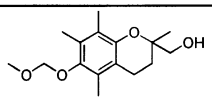 | Co-injection | Process Intermediate |
| **11** | 13.7 | 234 | 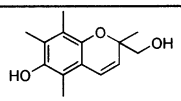 | Comparison with authentic sample | Byproduct |
| **9** | 17.0 | 441 | 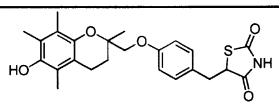 | | Parent |
| **5** | 29.0 | 358 | 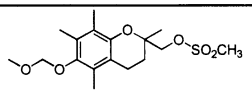 | Co-injection | Process Intermediate |
| **12** | 27.0 | 356 | 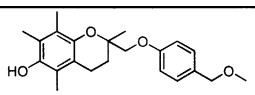 | NMR & MS data | Byproduct |
| **13** | 34.0 | 398 | 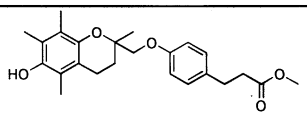 | NMR & MS data | Degradation product |

layer is separated and the aq. layer is extracted with dichloromethane. The combined organic layer is concentrated to afford an impure sample of the unsaturated compound **11** (9 g; yield: 89%). The spectral data of the impure sample were found to be informative enough to conclude that the impurity present in troglitazone was in fact the same as prepared above.

### 3.4. Chromatography for the isolation of impurities *12* and *13*

#### 3.4.1. Column chromatography

The methanol mother liquors were adsorbed on silica gel (60–120-mesh) and loaded on a column packed with the same mesh silica gel. The least polar fractions were collected to obtain a highly enriched mixture of compounds **12** and **13**, which were used for isolating the two compounds by preparative HPLC.

#### 3.4.2. Preparative HPLC

The above-obtained enriched mixture was subjected to preparative HPLC using the following conditions. The preparative HPLC system equipped with LC pump (Model LC-8A), Rheodyne injector (7125) with 2 ml loop capacity, UV/Vis spectrophotometric detector (SPD-6AV), Fraction collector (FCV-100B) and C-R7A Chromatopack monitor, all of Shimadzu make, were utilized. The preparative HPLC chromatogram showed target impurities **12** and **13** at 27.0 and 34.0 min, respectively. Fractions of these compounds were collected through repeated injections, pooled together and concentrated. Column, Hypersil prep. ODS $250 \times 10$ mm$^2$, 8 μm; mobile phase, 0.025 M $CH_3COONH_4$:$CH_3CN$:$CH_3OH$ (35:55:12), pH 4.5; flow rate, 2 ml/min; detection: UV at $\lambda = 230$ nm.

## 4. Results and discussion

### 4.1. LC–MS analysis of troglitazone

Mother liquor containing the impurities along with troglitazone was subjected to LC–MS analysis using the solvent system as described in Section 2.3.1. In this solvent system, troglitazone eluted at 17.0 min with a molecular ion at $m/z = 441$ (see Table 1). The structures of polar and non-polar impurities have been tentatively identified by molecular ion information obtained by LC–MS data. The structures of these impurities were confirmed by synthesis, NMR and single-crystal X-ray diffraction studies. The formation and characterization of these impurities are presented in this section.

### 4.2. Formation and characterization of impurities

#### 4.2.1. Process-related impurities *2*–*5*

The polar impurities hydroxy ester **2**, diol **3**, MOM-protected alcohol **4** and the non-polar impurity, viz. MOM-protected mesylate **5** have been identified to be present in the final compound and these intermediates have been confirmed by means of co-injection with reference samples in HPLC.

#### 4.2.2. By-products and degradation impurities

The impurities **10**–**12** are by-products in the process, whereas impurity **13** could be due to the degradation of troglitazone (**9**). Impurities **10** and **11** could be assigned based on the mass spectral fragmentation and by comparison with the samples prepared by design. Based on mass spectral data alone, the structure of compounds **12** and **13** could not be deduced and hence these compounds were isolated by preparative HPLC. NMR and/or X-ray diffraction studies were undertaken on the isolated samples.

#### 4.2.3. Formation of impurity *10*

The MOM-protected mesylate **5** can undergo deprotection of MOM group under acidic conditions to give the free hydroxy impurity **2**, as shown in Fig. 2.

The mass spectrum of compound **10** obtained by the LC–MS analysis, displayed a molecular ion at $m/z = 314$ corresponding to the molecular formula $C_{15}H_{22}O_5S$. The fragmentation pattern ($m/z = 91$, 121, 165, 203, 205) matched very well with that of compound **3** in which the secondary hydroxyl group is not protected by mesylate group. It is interesting to note that both compounds have the

same base peak at $m/z = 165$ corresponding to the ion (**14**) (Fig. 3). This stable ion could be formed by the aromatic ring expansion of chromenol moiety. Unambiguous support came by comparing the retention time in HPLC and co-injecting a sample of compound **10** prepared from compound **5** by deprotecting the MOM group under reported conditions [5].

#### 4.2.4. Formation of impurity *11*

Compound **3** loses a molecule of hydrogen to afford the unsaturated compound **11**, as shown in Fig. 4, and this transformation could be driven as the product is favored because of extended conjugation.

The mass spectrum of compound **11** obtained by the LC–MS analysis displayed a molecular ion at $m/z = 234$ corresponding to the molecular formula $C_{14}H_{18}O_3$. The fragmentation pattern of compound **11** is compared with that of compound **3**. The spectrum showed a base peak at $m/z = 189$, corresponding to the ion (**15**). The base peak could be attributed to the stability achieved by the extended conjugation. If the double bond was not present in ring B of compound **11**, the base peak could have been $m/z = 165$. Hence the base peak at $m/z = 189$ further lends support to the proposed structure. However, unambiguous support came by comparing the spectral data of **11** with those of an authentic compound prepared by the bleach oxidation [6] of diol **3**. $^1$H NMR showing the two doublets corresponding to α,β-unsaturation apart from the superimposable mass spectral fragmentation pattern lend support to the structure. The shift in $\lambda_{max}$ in the UV spectrum of the unsaturated compound **11** ($\lambda_{max} = 235$ nm) compared with that in diol **3** ($\lambda_{max} = 265$ nm) clearly indicates that there is an extended conjugation in **11** (Fig. 4).

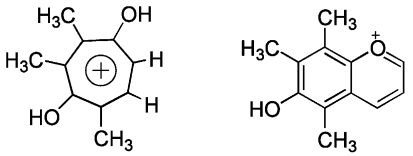


**14**: m/z 165 **15**: m/z 189

Fig. 3. Fragment ions in impurities **10** and **11**.

#### 4.2.5. Formation of impurity *12*

The MOM-protected aldehyde **6** under acidic conditions gets deprotected to give the hydroxy aldehyde **16**, which in turn gets reduced with Mg/MeOH to yield alcohol **17**. Alcohol **17** is methylated due to the presence of methanol in the reaction mixture to give impurity **12**, as shown in Fig. 5.

This impurity **12** has been isolated by means of preparative HPLC. The mass spectrum displayed the molecular ion at $m/z = 356$ corresponding to the molecular formula $C_{22}H_{28}O_4$. $^1$H NMR spectrum showed methyl singlets at $\delta = 1.5$ (3H), 2.15 (6H) and 2.2 (3H). The methylene protons at $\delta = 2.7$ (t, $J = 5.0$ Hz) is coupled (as shown by COSY) to another pro-chiral methylene protons at $\delta = 2.2$ (m) and 1.9 (m). $^{13}$C NMR and DEPT spectra identified four methyl carbons at $\delta = 11.22$, 11.74, 12.14 (attached to aromatic ring) and 22.72 (angular methyl). The spectrum also showed methylene carbon resonances at $\delta = 28.70$ (benzylic) and 20.28. The quaternary carbons were identified at 145.05, 144.92, 122.56, 121.45, 118.75, 117.26 and 74.24. The third methylene (pro-chiral) resonated at $\delta = 3.95$ (AB quartet $J = 9.0$ Hz) and the corresponding carbon was observed at $\delta = 72.65$. The above data are comparable with those of 2-hydroxymethyl-2,5,7,8-tetramethyl-3,4-dihydro-6-chromenol moiety.

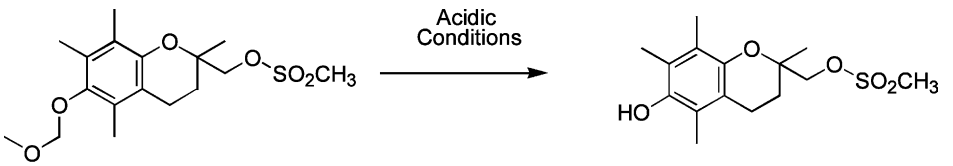


**5** **10**

Fig. 2. Formation of impurity **2**.

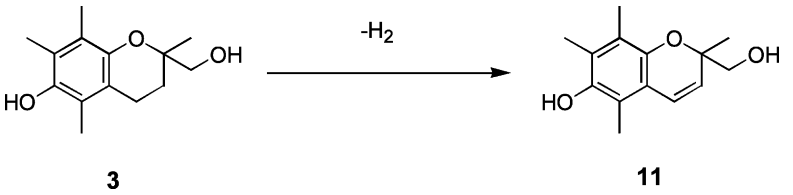


Fig. 4. Formation of impurity **11**.

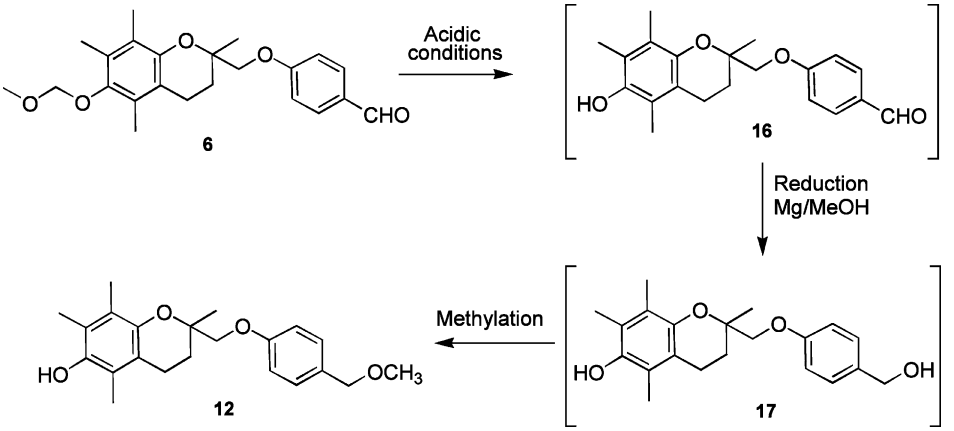


Fig. 5. Formation of impurity **12**.

$^{1}$H NMR spectrum also displayed aromatic signals at $\delta = 7.25$ (2H, d, $J = 8.2$ Hz) and 6.95 (2H, d, $J = 8.2$ Hz), one methylene signal at $\delta =$ 4.45 (2H, s) and one methyl signal at $\delta = 3.4$ (3H, s). $^{13}$C NMR spectrum displayed aromatic resonances at 158.79 (q), 130.31 (q), 129.28 (2CH) and 114.58 (2CH), one methylene at 74.24 and a methyl at 57.59. These NMR signals indicate the presence of *p*-hydroxyphenylmethyl methyl ether moiety. DQF-COSY and HETCOR experiment were performed to identify the $^{1}$H–$^{1}$H and $^{13}$C–$^{1}$H coupling. The long-range HETCOR experiment helped in the assignment of quaternary carbons and the C–C–C–H correlations are shown in Fig. 6. NMR assignments are listed in Table 2.

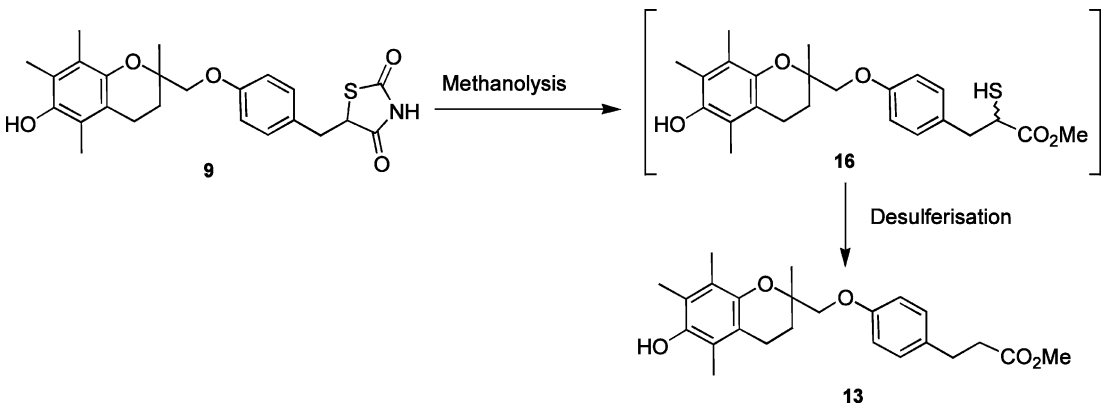


Fig. 6. Formation of impurity **13**.

Table 2

| Position | $^1$H | $\delta$ (ppm) | $J$ (Hz) | COSY | $^{13}$C | DEPT | HETCOR |
|---|---|---|---|---|---|---|---|
| 1 | – | – | – | – | 145.05 | – | – |
| 2 | – | – | – | – | 118.75 | – | – |
| 3 | – | – | – | – | 121.45 | – | – |
| 4 | – | – | – | – | 144.92 | – | – |
| 5 | – | – | – | – | 122.56 | – | – |
| 6 | – | – | – | – | 117.26 | – | – |
| 7 | 1H | 5.8 | s | – | – | – | – |
| 8 | 3H | 2.15 | s | – | 12.15 | $CH_3$ | (8H, 2.15) |
| 9 | 3H | 2.15 | s | – | 11.74 | $CH_3$ | (9H, 2.15) |
| 10 | 3H | 2.2 | s | – | 11.22 | $CH_3$ | (10H, 2.2) |
| 12 | 2H | 2.7 | t, 5.0 | (13Ha, 2.2), (13Hb, 1.9) | 20.28 | $CH_2$ | (12H, 2.7) |
| 13 | Ha | 2.2 | m | (13Hb, 1.9), (12H, 2.7) | 28.70 | $CH_2$ | (13Ha, 2.2) |
| | Hb | 1.9 | m | (13Ha, 2.2), (12H, 2.7) | | | (13Hb, 1.9) |
| 14 | – | | – | – | 74.24 | – | – |
| 15 | 3H | 1.5 | s | – | 22.72 | $CH_3$ | (15H, 1.5) |
| 16 | 2H | 3.9 | AB q, 9.0 | – | 72.65 | $CH_2$ | (16H, 3.9) |
| 18 | – | | – | – | 158.79 | – | – |
| 19 | 1H | 7.25 | d, 8.2 | – | 114.58 | CH | (19H, 7.25) |
| 20 | 1H | 6.95 | d, 8.2 | – | 129.26 | CH | (20H, 6.95) |
| 21 | – | – | – | – | 130.31 | – | – |
| 22 | 1H | 6.95 | d, 8.2 | – | 129.26 | CH | (22H, 6.95) |
| 23 | 1H | 7.25 | d, 8.2 | – | 114.58 | CH | (23H, 7.25) |
| 24 | 2H | 4.45 | s | – | 74.24 | $CH_2$ | (24H, 4.45) |
| 26 | 3H | 3.4 | s | – | 57.59 | $CH_3$ | (26H, 3.4) |

Refer structural formula for numbering (Fig. 7).

*4.2.6. Formation of impurity **13***

Methanolysis of troglitazone **9** gives mercaptan **16**, which on desulpherization affords impurity **13**, as shown in Fig. 7. Thiazolidinedione is vulnerable to such conditions and it is reasonable to expect the formation of the said impurity.

The mass spectrum displayed the molecular ion at $m/z = 398$ corresponding to the molecular formula $C_{24}H_{30}O_5$. $^1$H NMR spectrum showed methyl singlets at $\delta = 1.45$ (3H), 2.15 (6H) and 2.2 (3H). The methylene protons at $\delta = 2.7$ are coupled (as shown by COSY) to the pro-chiral methylene protons at $\delta = 2.2$ (m) and 1.9 (m), respectively. $^{13}$C NMR and DEPT spectra identified four methyl carbons at $\delta = 11.05$, 11.57, 11.97 (attached to aromatic ring) and 22.57 (angular

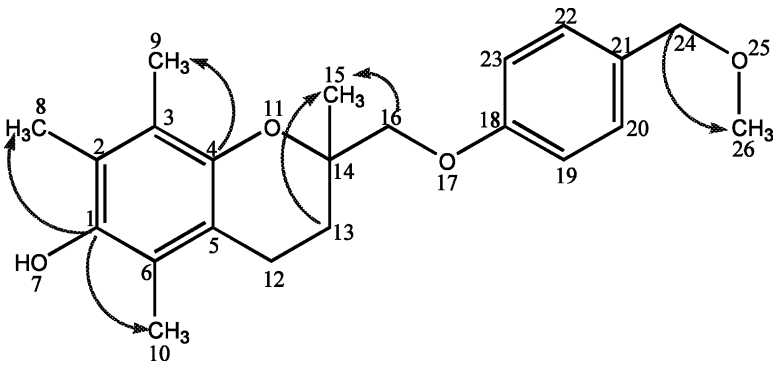


Fig. 7. C–C–C–H correlations of impurity **12**.

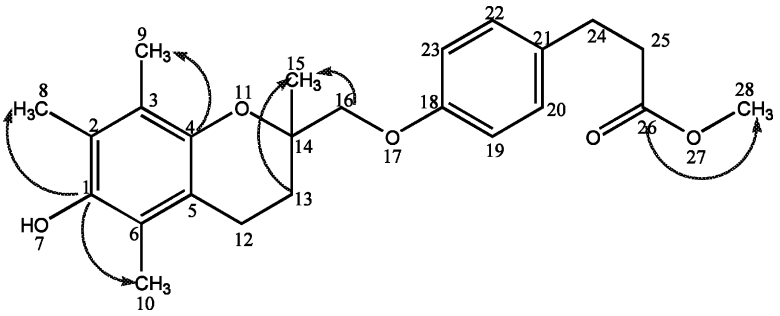


Fig. 8. C–C–C–H correlations in impurity **13**.

methyl). The spectrum also showed methylene carbon resonances at $\delta = 28.54$ (benzylic) and 20.12. The quaternary carbons were identified at 145.03, 144.86, 122.50, 121.32, 118.60, 117.21 and 73.96. The third methylene (pro-chiral) resonated at $\delta = 3.95$ (AB quartet $J = 9.0$ Hz) and the corresponding carbon was observed at $\delta = 72.53$. The above data are comparable with those of 2-hydroxymethyl-2,5,7,8-tetramethyl-3,4-dihydro-6-chromenol moiety. $^{1}$H NMR spectrum also displayed aromatic signals at $\delta = 7.15$ (2H, d, $J = 8.0$ Hz) and 6.85 (2H, d, $J = 8.0$ Hz), two methylene signals at $\delta = 2.90$ (2H, t, $J = 7.6$ Hz), 2.65 (2H, t, $J = 7.6$ Hz), and one methyl signal at $\delta = 3.7$ (3H, s). $^{13}$C NMR spectrum displayed resonances at 173.43 (q), 157.58 (q), 132.66 (q), 129.03 (2CH)

Table 3

| Position | $^{1}$H | $\delta$ (ppm) | $J$ (Hz) | COSY | $^{13}$C | DEPT | HETCOR |
|---|---|---|---|---|---|---|---|
| 1 | – | – | – | – | 145.03 | – | – |
| 2 | – | – | – | – | 118.60 | – | – |
| 3 | – | – | – | – | 121.32 | – | – |
| 4 | – | – | – | – | 144.86 | – | – |
| 5 | – | – | – | – | 122.50 | – | – |
| 6 | – | – | – | – | 117.21 | – | – |
| 7 | 1H | 4.90 | s | – | – | – | – |
| 8 | 3H | 2.15 | s | – | 11.97 | $CH_3$ | (8H, 2.15) |
| 9 | 3H | 2.15 | s | – | 11.57 | $CH_3$ | (9H, 2.15) |
| 10 | 3H | 2.20 | s | – | 11.05 | $CH_3$ | (10H, 2.2) |
| 12 | 2H | 2.7 | – | (13Ha, 2.2), (13Hb, 1.9) | 20.12 | $CH_2$ | (12H, 2.7) |
| 13 | Ha | 2.2 | m | (13Hb, 1.9), (12H, 2.7) | 28.54 | $CH_2$ | (13Ha, 2.2) |
| | Hb | 1.9 | m | (13Ha, 2.2), (12H, 2.7) | | | (13Hb, 1.9) |
| 14 | – | | – | – | 73.96 | – | – |
| 15 | 3H | 1.45 | s | – | 22.57 | $CH_3$ | (15H, 1.45) |
| 16 | 2H | 3.95 | AB q, 9.0 | – | 72.53 | $CH_2$ | (16H, 3.95) |
| 18 | – | | – | – | 157.58 | – | – |
| 19 | 1H | 7.15 | d, 8.0 | – | 114.65 | CH | (19H, 7.15) |
| 20 | 1H | 6.85 | d, 8.0 | – | 129.03 | CH | (20H, 6.85) |
| 21 | – | – | – | – | 132.66 | – | – |
| 22 | 1H | 6.85 | d, 8.0 | – | 129.03 | CH | (22H, 6.85) |
| 23 | 1H | 7.15 | d, 8.0 | – | 114.65 | CH | (23H, 7.15) |
| 24 | 2H | 3.9 | t, 7.6 | (25H, 2.6) | 35.79 | $CH_2$ | (24H, 3.9) |
| 25 | 2H | 2.6 | t, 7.6 | (24H, 3.9) | 29.89 | $CH_2$ | (25H, 2.6) |
| 26 | – | – | – | – | 173.43 | – | – |
| 28 | 3H | 3.7 | s | – | 51.39 | $CH_3$ | (28H, 3.7) |

Refer structural formula for numbering (Fig. 8).

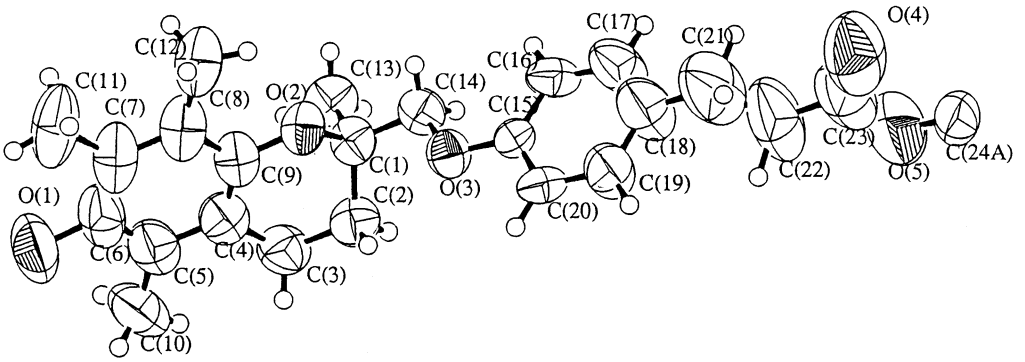


Fig. 9. ORTEP diagram of impurity **13**.

and 114.56 (2CH), one methylene at 35.79, 29.89 and a methyl at 51.39. These NMR signals indicate the presence of methyl ester of *p*-hydroxyphenyl propionic acid moiety. DQF-COSY and HETCOR experiment were performed to identify the $^{1}H-^{1}H$ and $^{13}C-^{1}H$ coupling. The long-range HETCOR experiment helped in the assignment of quaternary carbons and the C–C–C–H correlations are shown in Fig. 8. NMR assignments are listed in Table 3. The structure of this compound has been confirmed unambiguously by means of single-crystal X-ray diffraction studies [7] and the ORTEP drawing is shown in Fig. 9. The molecule crystallizes as a hemihydrate. The oxygen O(5) atom of the ester group has hydrogen bond contact with the lattice water molecule. Chroman ring assumes a half-chair conformation, while the central aromatic ring is nearly perpendicular to the aromatic ring of the chroman moeity. The terminal ester group is disordered.

## 5. Conclusions

The impurity profile study of troglitazone has been carried out primarily by LC–MS. The four process-related impurities (**2**–**5**) have been detected by LC–MS and were confirmed by co-injection with authentic samples. Apart from the process-related impurities, two polar by-products (**10** and **11**) were characterized by mass spectral data and comparison with reference samples, while one non-polar by-product (**12**) and one degradation product (**13**) have been isolated by means of preparative HPLC and characterized by 2D NMR and mass spectral study. Single-crystal X-ray diffraction studies have been carried out on the degradation product (**13**). The formation and characterization of these by-products and degradation product have been discussed.

## Acknowledgements

The authors wish to thank the management of Dr. Reddy's Research Foundation for permitting this work to be published. Cooperation extended by all the colleagues of Process and Analytical R&D divisions, particularly Mr. D. Sreenivas Rao and Mr. U. Satyanarayana, is gratefully acknowledged.

## References

[1] H. Horikoshi, T. Yoshioka, T. Kawasaki, K. Nakamura, N. Matsunuma, N.K. Yamaguchi, K. Sasahara, Annu. Rep. Sankyo Res. Lab. 46 (1994) 1.

[2] (a) K. Vyas, C. Prabhakar, D.S. Rao, M.R. Sarma, G. Om Reddy, R. Rajagopalan, R. Chakrabarti, PCT/WO-97/27191.;
(b) K. Vyas, C. Prabhakar, D.S. Rao, M.R. Sarma, G. Om Reddy, R. Rajagopalan, R. Chakrabarti, US Patent 5 700 870.

[3] (a) C. Prabhakar, G. Madhusudhan, K. Sahadev, Ch.M. Reddy, M.R. Sarma, G. Om Reddy, R. Chakrabarti, C.S. Rao, T.D. Kumar, R. Rajagopalan, Biorg. Med. Chem. Lett. 8 (1998) 2725;
(b) B.B. Lohray, V. Bhushan, P.B. Rao, G.R. Madhavan, N. Murali, K.N. Rao, K.A. Reddy, B.M. Rajesh, P.G.

Reddy, R. Chakrabarti, R. Rajagopalan, Biorg. Med. Chem. Lett. 7 (1997) 785.
[4] T. Takebayashi, T. Onodera, K. Hasegawa, T. Fujita, T. Yoshioka, EP 454 501.
[5] J.P. Yardley, H. Fletcher, Synthesis (1976) 244.
[6] M.R. Leanna, T.J. Sowin, H.E. Morton, Tetrahedron Lett. 33 (1992) 5029 (See for a typical TEMPO/Bleach oxidation procedure).
[7] X-ray data of **13**: $C_{24}H_{30}O_5$, triclinic, space group *P1*, $a = 12.109$ (1), $b = 15.458$ (2), $c = 5.967$ (1) Å, $\alpha = 95.777$ (1), $\beta = 99.73$ (1), $\gamma = 91.38$ (1), $V = 1094.3$ (2) Å$^3$, $Z = 2$. Intensity data were collected on a Rigaku AFC7S diffractometer in the $\omega/2\theta$ scan mode. The intensity data were corrected for Lorentz polarization. The structure was solved by direct methods (SIR 92) and refined by least-square procedure. The present *R* factor is 16.6% for 2385 observed reflections ($I > 1.5\sigma(I)$).